

Research Paper

Platelet-Rich Plasma Injection in Burn Scar Areas Alleviates Neuropathic Scar Pain

Shu-Hung Huang^{1,2,3,4,5}; Sheng-Hua Wu^{6,7,8}; Su-Shin Lee^{1,2,3,4}; Yun-Nan Lin^{1,2}; Chee-Yin Chai⁹; Chung-Sheng Lai^{1,2}; Hui-Min David Wang^{3,10}✉

1. Division of Plastic Surgery, Department of Surgery, Kaohsiung Medical University Hospital, Kaohsiung, Taiwan
2. Department of Surgery, School of Medicine, College of Medicine, Kaohsiung Medical University, Kaohsiung, Taiwan
3. Center for Stem Cell Research, Kaohsiung Medical University, Kaohsiung, Taiwan
4. Orthopaedic Research Center, Kaohsiung Medical University, Kaohsiung, Taiwan
5. Graduate Institute of Medicine, College of Medicine, Kaohsiung Medical University, Kaohsiung, Taiwan
6. Department of Anesthesiology, Kaohsiung Medical University Hospital, Kaohsiung, Taiwan
7. Department of Anesthesiology, Kaohsiung Municipal Hsiao-Kang Hospital, Kaohsiung, Taiwan
8. Department of Anesthesiology, School of Medicine, College of Medicine, Kaohsiung Medical University, Kaohsiung, Taiwan
9. Department of Pathology, Kaohsiung Medical University Hospital, Kaohsiung, Taiwan
10. Graduate Institute of Biomedical Engineering, National Chung Hsing University, Taichung 402, Taiwan

✉ Corresponding author: Hui-Min David Wang, Ph.D. Professor, Graduate Institute of Biomedical Engineering, National Chung Hsing University, Taichung 402, Taiwan. Address: No.145, Xingda Rd., South Dist., Taichung City 402, Taiwan. Mobil: 886-935753718; TEL: 886-4-22873181-360#732; Fax: 886-4-22852242; E-mail: davidw@dargon.nchu.edu.tw

© Ivyspring International Publisher. This is an open access article distributed under the terms of the Creative Commons Attribution (CC BY-NC) license (<https://creativecommons.org/licenses/by-nc/4.0/>). See <http://ivyspring.com/terms> for full terms and conditions.

Received: 2017.08.27; Accepted: 2017.12.11; Published: 2018.01.08

Abstract

Objective: No effective treatments have yet been developed for burn-induced neuropathic pain. Platelet-rich plasma (PRP) has been reported to ameliorate various types of inflammation pain. However, the effect of PRP on burn-induced neuropathic pain is unclear.

Methods: Burn-induced neuropathic pain Sprague-Dawley rat model was confirmed using a mechanical response test 4 weeks after the burn injuries were sustained, following which PRP was injected in the scar area. The rats were divided into four groups (n = 6) as following: Group A, Sham; Group B, Sham + PRP; Group C, Burn; and Group D, Burn + PRP. Four weeks after the PRP injection, the animals were subjected to behavior tests and then sacrificed; specimens were collected for inflammation tests, Masson's trichrome stain and chromosome 10 (PTEN) in the injured skin; and PTEN, phosphorylated mammalian target of rapamycin (p-mTOR), p38, nuclear factor κB (NFκB), chemokine (CC motif) ligand 2 (CCL2), and CCL2 cognate receptor (CCR2) in spinal cord dorsal horns through immunohistochemistry and immunofluorescence staining.

Results: PRP significantly alleviated allodynia in burn-induced neuropathic pain 4 weeks after treatment, and PTEN expression in the skin and spinal cord were significantly increased in group D compared with the group C. p-PTEN, p-mTOR, and CCL2 expression in neuron cells; p-p38 and p-NFκB expression in microglia; and p-JNK and p-NFκB activation in spinal astrocytes decreased significantly in the group D compared with the group C.

Conclusions: PRP is effective in treating burn-induced neuropathic pain and may be used in clinical practice.

Key words: PRP, Burn, Scar, Neuropathic Pain

Introduction

Each year, nearly 11 million individuals worldwide require medical treatment for burn injuries[1]. More than 50% of these patients experience neuropathic pain[2, 3], which can persist for years[4, 5]. Neuropathic pain is a complex, chronic

pain status for which no consensus has been reached regarding the optimal therapy; current approaches include neural blockade, pharmacotherapy, and local anesthetics[6, 7].

A recent rat study reported that chronic

constriction injuries can downregulate spinal phosphatase and tensin homologue deleted on chromosome 10 (PTEN) as well as upregulate the phosphorylation of the mammalian target of rapamycin (mTOR) and tumor necrosis factor- α (TNF- α), resulting in neuroinflammation[8]. Neuropathic pain is processed as neuroinflammation, and the interaction between neurons, microglia, and astrocytes thus creates a vicious cycle that sustains this chronic pain[9]. Chronic pain through neuron-glia interaction entails the activation of microglia and astrocytes[10, 11]. Microglial activation results in the activations of p-p38 and nuclear factor κ B (NF κ B) signaling pathways, and the production of inflammatory mediators, including TNF- α , interleukin-1 β (IL-1 β), and IL-18[9]. Guo *et al.* [12] reported that IL-1 β and chemokine (CC motif) ligand 2 (CCL2)-CCL2 cognate receptor (CCR2) signaling cascades played an important role in neuron-glia-cytokine interactions and facilitate neuropathic pain. Furthermore, literatures were pointed out that neutralizing CCL2 attenuates neuropathic pain [12, 13]. Burn injury damages skin as well as nerve endings through neuroinflammation; spinal cord astrocyte and microglial activation; PTEN downregulation; p-mTOR upregulation; and increased p-p38 and NF κ B, IL-1 β , and CCL2 expression in the spinal cord region.

Proteomics studies have shown that the platelet-rich plasma (PRP) contain more than 1,100 various peptides, including enzymes, enzyme inhibitors, growth factors, and immune system messengers; these proteins may have anti-inflammatory, neuropathic pain control, and tissue repair activities[14, 15, 16]. Therefore, PRP has the potential to decrease pain through the effects of these bioactive molecules and growth factors[17]. PRP has been used extensively in various pain conditions, such as muscle injury, knee osteoarthritis pain[17], tendinopathy and traumatic neuropathic pain[18, 19, 20]. However, no studies have reported on the effectiveness of PRP in treating burn-induced neuropathic pain. The main aim of our study was to survey the PRP effect on burn-induced neuropathic pain, and assess expression of PTEN in the burn skin and spinal cord, mTOR, pp38, CCL2 and CCR2 immunofluorescence activity in the spinal cord after PRP treatment.

Materials and Methods

Model of burn-induced neuropathic pain and behavior test

Rats (Sprague Dawley, male, 180–200 g weight) were fed a standard laboratory diet. All animal

investigational protocols were approved by the institutional animal care and use committee of Kaohsiung Medical University (approval no. 104037). The rats were divided into four groups (n = 6, in each group) as following: Group A, sham; Group B, sham + PRP; Group C, burn; and Group D, burn + PRP. Figure 1 presents the experimental flow chart. A burn-induced neuropathic pain model was established as described previously[21]. In brief, a third-degree burn injury was induced in anesthetized rats by placing the right hind paw on a 75°C \pm 0.5°C heated metal block with a water bath, with a 100g weight on the paw, for 10 seconds. The wound was treated with silver sulfadiazine cream every day till wound healing (approximately 3-4 weeks). Paw withdrawal latencies (PWLs) and paw withdrawal thresholds (PWTs) were performed as reported in our previous study (Figure 1).

Preparation of PRP

To prepare PRP as following the manufacture's manual. Briefly, 12 mL of whole blood was extracted from the heart and placed in a PRP centrifuge tube 50ml (AesMed Co., Ltd., Taipei, Taiwan) containing 1.8 mL of acid citrate dextrose solution (AesMed Co., Ltd., Taipei, Taiwan) and centrifuged at 3,000 rpm for 4 minutes. Then, approximately 1.5 mL of PRP was collected at the middle range of the PRP tube. In order to minimize the variation, PRP from six rats were mixed together. Subsequently, 1.5 mL of calcium chloride (100 mg/mL; AesMed Co., Ltd., Taipei, Taiwan) was added to activate the 1.5ml PRP. 0.4 mL of the activated PRP was subcutaneously injected into the burn-injured hind paw by using a 26-gauge needle.

Complete blood count examination and enzyme-linked immunosorbent assay (ELISA) on PRP and plasma

The white blood cell, platelet, lymphocyte, neutrophil, monocyte, and red blood cell counts of the PRP and plasma were measured using a blood analyzer (Advia 2120, Bayer); as described in our previous study[22], several growth factors were detected using an enzyme-linked immunosorbent assay (ELISA). The standard curve was obtained for each experiment. Platelet-derived growth factor (PDGF) AA, PDGF BB (RayBiotech Co., Georgia, USA), epidermal growth factor (EGF), and vascular epidermal growth factor (VEGF; Koma Co., Republic of Korea) levels were quantitatively measured using ELISA kits, with reference range was from 0 to 3000 (PDGF AA), from 0 to 2000 (PDGF BB), from 0 to 1000 (EGF) and from 0 to 1000 (VEGF) pg/ml, respectively. All measurements were conducted in triplicate.

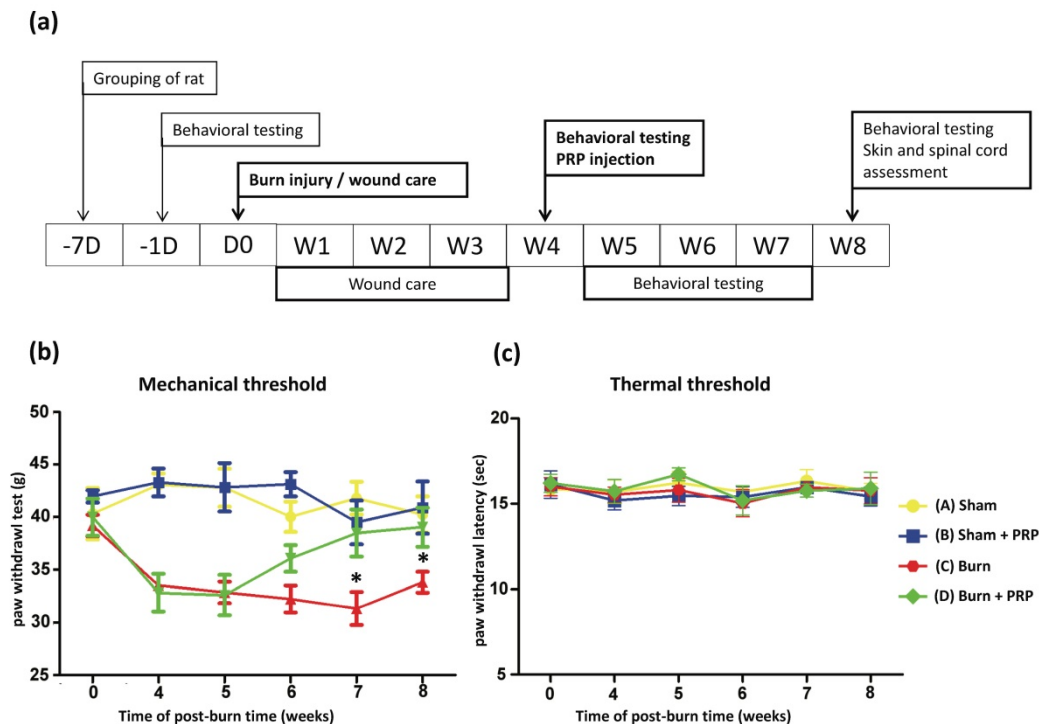


Figure 1. Study outline and behavior test results over time. (Top) Study flowchart: D, day, W, week. (Bottom, left) Compared with the burn group, response thresholds to mechanical stimuli in the Burn + PRP group significantly increased at weeks 7 and 8 (data are plotted as mean \pm SEM * $p < 0.05$). (Bottom, right) Radiant heat stimuli of the two groups did not differ significantly.

Western blot analysis

The procedures were the same as our previous reports[22]. The rats were sacrificed 4 weeks after PRP or vehicle treatment. The hind paw skins were harvested and divided into two parts for tissue staining and detecting protein level expression. The skins were homogenized in T-PER® (Thermo Fisher Scientific Co., Oklahoma, USA) containing a protease cocktail inhibitor, and the supernatants obtained after centrifuging at 13,000 rpm for 30 minutes at 4°C were applied to determine the protein expressions. An equal amount of protein samples was separated on SDS-polyacrylamide gel, and the separated proteins were transferred onto a polyvinylidene difluoride membrane and blocked with a blocking solution (5% nonfat milk) for 1 hour. Then, the membrane was incubated overnight at 4°C with a primary PTEN antibody (1:1000 dilution; Cell Signaling Technology, Danvers, MA, USA). Subsequently, the membrane was washed 3 times with TBST. The washed membranes were incubated with a horseradish peroxidase (HRP) conjugated secondary antibody (1:5000 dilution) and visualized through enhanced chemiluminescence. The relative band densities were recorded using a Bio-Rad ChemiDoc XRS system and quantified using Quantity One software. Equal loading of protein was confirmed by measuring β -actin expression.

Immunohistochemistry and Masson trichrome staining

Specimens were harvested 4 weeks after PRP treatment in all groups. The hind paw skin was harvested and fixed in formalin and embedded in paraffin; then, 4- μ m-thick skin sections were cut and mounted on glass slides, and then deparaffinized and tissue rehydrated in graded alcohol solutions. The sections were subjected to antigen to heat-induced antigen retrieval by heating them to 121°C in 0.1 mol/L of citrate buffer (10mM citrate butter pH 6.0) in an autoclave for 10 minutes and then was cooled naturally to room temperature. Next, endogenous peroxidase activity was quenched by 3% H₂O₂ for 5 minutes. Nonspecific sites are blocked by 5% goat serum in phosphate-buffered saline for 30 minutes, the sections were then incubated with a rabbit polyclonal antibody against PTEN (1:200; Cell Signaling Technology, MA) for 1 hour at room temperature. The sections were then incubated for 30 minutes at room temperature with a secondary antibody conjugated with HRP. Finally, the slides were incubated in 3,3-diami-nobenzidine for 5 minutes and subjected to Mayer hematoxylin counterstaining for 60 s. The skin sections were then subjected to Masson trichrome staining per the routine histologic protocol[21]. The percentage of collagen deposition and the number of cells per

high-power view in the skin tissue were quantified using Image-Pro Plus Version 6.0 software (Media Cybernetics, Inc., Rockville, MD, USA).

Immunofluorescence staining

The lumbar spinal cord segments were harvested 4 weeks after PRP or vehicle treatment. The fresh-frozen sections were prepared and cut into 16-mm slides for immunofluorescence staining. For double immunofluorescence staining as our previous reports[22], spinal cord dorsal horns were incubated with a mix of polyclonal p-PTEN (1:200 dilution; Cell Signaling Technology) and monoclonal NeuN (a neuron cell marker; 1:1000; Millipore, Temecula, CA, USA), polyclonal PTEN (1:200 dilution; Cell Signaling Technology) and monoclonal NeuN, polyclonal p-mTOR (1:200 dilution; Cell Signaling Technology; Boston, MA, USA) and monoclonal NeuN, polyclonal mTOR (1:200 dilution; Cell Signaling Technology, Boston) and monoclonal NeuN, polyclonal p-p38 (1:200 dilution; Cell Signaling Technology, Massachusetts, USA) and monoclonal OX42 (a microglia marker; 1:200; Serotec, Raleigh, NC, USA), polyclonal pNF κ B (1:200 dilution; Cell Signaling Technology, Boston) and monoclonal OX42, polyclonal CCL2 (1:200 dilution; Cell Signaling Technology, Boston) and monoclonal NeuN, polyclonal CCR2 (1:200 dilution, Cell Signaling Technology, Boston) and monoclonal NeuN, polyclonal pNF κ B and monoclonal GFAP (an astrocyte marker; 1:1000 dilution; BD Biosciences San Diego, CA, USA), and p-JNK (1:200 dilution; Cell Signaling Technology, Boston) and monoclonal GFAP overnight at 4°C. The appropriate secondary antibody conjugated with goat anti-rabbit Cy3 (Jackson ImmunoResearch, West Grove, PA, USA) and goat anti-mouse FITC (Jackson ImmunoResearch) was added. Images were acquired using a fluorescence microscope (Leica DMI6000).

Statistical analysis

Statistical analysis was performed using Statistical Package for the Social Sciences (SPSS, Inc., Chicago, IL, USA) version 14.0. Each sample was measured in triplicate, and data were recorded as mean \pm standard error of the mean (SEM; rat, n = 6 in each group). Cytokines and growth factors in the PRP were analyzed by one-way ANOVA and Tukey pairwise comparison, with $p < .05$ representing statistical significance.

Results

PRP ameliorates burn-induced neuropathic pain at 3 weeks after the injection

The PWTs scores of rats with burn-induced mechanical allodynia significantly increased at 3

weeks after PRP injection. No significant changes were observed in the PWTs scores in the group A or in the group B (Figure 1, bottom panel). A marked decrease in the PWTs scores were noted 4 weeks after the burn injuries in group C and D. The PWTs scores increased significantly at 3 and 4 weeks after PRP injection (group D) compared with the group C. These results demonstrate that PRP can ameliorate burn-induced neuropathic pain.

Platelet count and PDGF aa/bb, VEGF, and EGF levels in PRP

The complete blood cell counts of PRP, plasma, and whole blood were compared. The platelet count was $3948.33 \pm 304.81 \times 10^3/\mu\text{L}$ in the PRP. The mean platelet count in the PRP was 6.20 \pm 0.29fold higher than that in the whole blood. The growth factor concentrations in PRP and plasma were measured through an ELISA. After PRP activation, PDGF AA, PDGF BB, VEGF, and EGF concentrations were 2609.08 ± 179.00 pg/mL, 82.78 ± 2.20 pg/m, 586.92 ± 13.84 pg/m, and 672.87 ± 1.47 pg/m, respectively (Table 1).

Table 1. Complete Blood Cell and Growth Factor Quantification of PRP, Plasma, and Whole Blood

Characteristic	PRP	Plasma	Whole blood	p-value
Normal CBC				
WBC (cell $\times 10^3/\mu\text{L}$)	1.58 \pm 0.06	1.84 \pm 0.6	2.43 \pm 0.85	
RBC (cell $\times 10^6/\mu\text{L}$)	0.00 \pm 0.00	0.04 \pm 0.01	7.67 \pm 0.23	
Lymphocyte (cell $\times 10^3/\mu\text{L}$)	1.39 \pm 0.04	1.62 \pm 0.08	1.61 \pm 0.46	
Neutrophils (cell $\times 10^3/\mu\text{L}$)	0.15 \pm 0.01	0.14 \pm 0.01	0.71 \pm 0.38	
Monocyte (cell $\times 10^3/\mu\text{L}$)	0.03 \pm 0.01	0.14 \pm 0.06	0.05 \pm 0.01	
PLT (cell $\times 10^3/\mu\text{L}$)	3948.33 \pm 304.81	1180.50 \pm 297.69	635.5 \pm 74.25	0.003**
Growth factor				
PDGF AA (pg/ml)	2609.08 \pm 179.00	487.32 \pm 15.75		0.049*
PDGF BB (pg/ml)	82.78 \pm 2.20	26.91 \pm 5.77		0.041*
VEGF (pg/ml)	586.92 \pm 13.84	290.31 \pm 14.31		0.032*
EGF (pg/ml)	672.87 \pm 1.47	365.88 \pm 2.07		0.017*

Values expressed as mean \pm SEM (n = 3)

CBC: complete blood count, WBC: white blood cell, RBC: red blood cell, PLT: platelet, PDGF: platelet-derived growth factor, EGF = epidermal growth factor, VEGF = vascular endothelial growth factor. * $p < 0.05$ in PRP vs plasma, ** $p < 0.01$ in PRP vs whole blood.

Subcutaneous PRP injection in burn scar areas reduced collagen deposition in dermal areas

After burn injury, the collagen amount was increased, and then deposited vertically and irregularly under hind paw skin (Figure 2). Four weeks after PRP injection, collagen deposition in the hind paw skin had decreased. In addition, compared with the group C, collagen fibers were more compact, parallel, and thinner in the group D.

Subcutaneous PRP injection increased PTEN immunoreactivity in hind paw skin and spinal cord dorsal horns and decreased mTOR immunoreactivity after burn injury

To explore the effect of hind paw burns on the PTEN pathway, PTEN immunoreactivity in the hind paw skin was quantified. The group C exhibited significantly decreased PTEN immunoreactivity after local PRP injection on the burned hind paw skin compared with the group A, B and D (group A 42.13% ± 4.44%; group B, 40.20% ± 5.52%; group C, 9.18% ± 4.2%; group D, 43.80% ± 9.43%; Figure 2).

To examine p-PTEN, PTEN, p-mTOR, and

mTOR immunoreactivity in the dorsal horn of the lumbar spinal cord, we subjected lumbar spinal tissue (L3-5) from all groups to double immunofluorescence staining. Spinal p-PTEN immunoreactivity in the group C and group D differed significantly (group C 17.32% ± 3.27% vs group D 5.06% ± 1.33%, *p* < 0.05; Figure 3). p-PTEN immunoreactivity increased after the burn injury and decreased after PRP injection. By contrast, spinal PTEN immunoreactivity significantly decreased in the group C, and after PRP injection, PTEN immunoreactivity increased significantly (group C 12.95% ± 3.61% vs group D 34.85% ± 2.14%, *p* < .05; Figure 3).

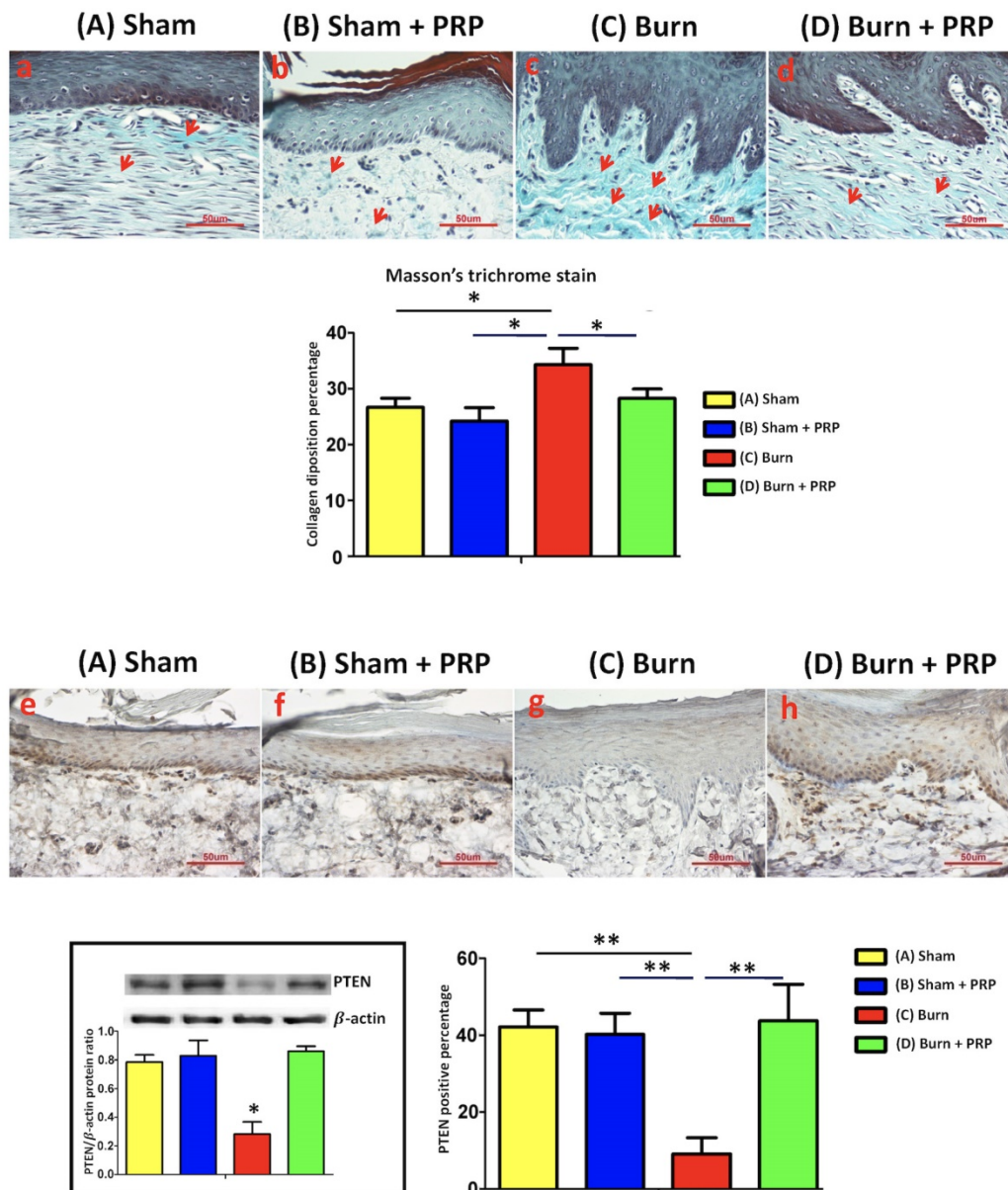


Figure 2. PRP decreased collagen deposition in burn-injured hindpaw skin and increased PTEN expression. (Top) Hind paw areas were treated with PRP and skin sections were harvested. Paraffin sections were cut and stained with Masson trichrome. In the burn group, hypertrophy and dense collagen bundles were found in the dermis. In the burn + PRP group, collagen deposition was significantly reduced compared with the burn group (**p* < 0.05). PRP upregulated PTEN expression in the burn-injured hind paw skin tissue (***p* < 0.01). Hind paw skin sections (10 μm) were harvested and stained 4 weeks after PRP injection. Scale bars in all images are 50 μm.

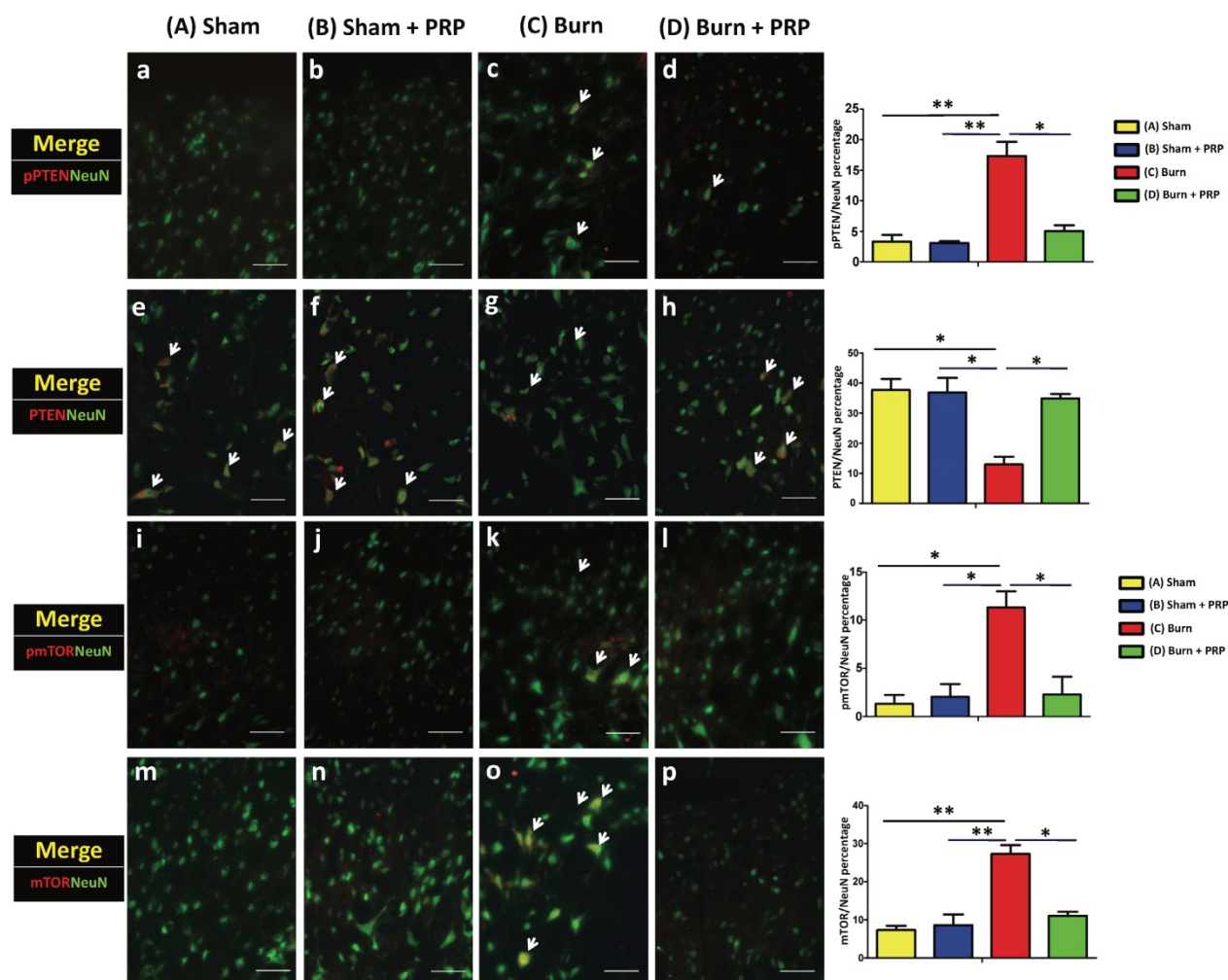


Figure 3. Subcutaneous PRP injection reduced p-PTEN and mTOR immunoreactivity in spinal cord dorsal horns. Spinal cord sections (10 μ m) were harvested 4 weeks after PRP injection. Immunostaining was performed for NeuN (green), PTEN (red), and mTOR (red). Spinal PTEN immunoreactivity decreased in the group C, and after PRP injection, PTEN immunoreactivity increased significantly (group C $12.95\% \pm 3.61\%$ vs group D $34.85\% \pm 2.14\%$, $p < .05$; Figure 3A). PRP reduced p-mTOR and mTOR immunoreactivity (group C $11.31\% \pm 2.38\%$ vs group D $2.56\% \pm 2.31\%$, $p < .05$, and group C $27.31\% \pm 3.27\%$ vs group D $11.06\% \pm 1.50\%$, $p < .05$, respectively; Figure 3B). Scale bars in all images are 50 μ m.

Burn injury in the hind paw skin increased p-mTOR and mTOR immunoreactivity in the spinal cord. PRP injection significantly decreased the p-mTOR and mTOR immunoreactivity (group C $11.31\% \pm 2.38\%$ vs group D $2.56\% \pm 2.31\%$, $p < .05$, and group C $27.31\% \pm 3.27\%$ vs group D $11.06\% \pm 1.50\%$, $p < .05$, respectively; Figure 3).

Confocal double immunostaining images of the lumbar spinal ventral horn further confirmed that most p-PTEN, PTEN, p-mTOR, and mTOR signals tended to localize with NeuN-positive neuron cells (Figure 3).

PRP subcutaneous injection decreased p-p38 and p-NF κ B immunoreactivity in spinal cord dorsal horns in burn-induced neuropathic pain model

To examine the effects of PRP on p-p38 and p-NF κ B activation in the spinal cord dorsal horns,

p-p38 and p-NF κ B (which are central sensitization and inflammation markers, respectively) were quantified through double immunofluorescence staining. The total number of p-p38 and OX42 double-positive cells in the group D decreased significantly compared with the group C (group C $40.76\% \pm 6.22\%$ vs group D $21.72\% \pm 1.11\%$, $p < .05$). Additionally, the number of p-NF κ B expressing microglia was significantly higher in the group C than in the group D (group C $21.96\% \pm 1.94\%$, group D $6.62\% \pm 1.51\%$, $p < 0.01$; Figure 4).

Subcutaneous PRP injection decreased CCL2 expression and increased CCR2 expression intensity in spinal cord dorsal horns in burn-induced neuropathic pain model

We examined CCL2 and CCR2 expression in spinal cord dorsal horns following burn injury with and without PRP subcutaneous injection. The

injection significantly decreased CCL2 immunoreactivity (group C $33.05 \pm 1.49\%$ vs group D $16.87\% \pm 1.86\%$, $p < .05$) and significantly increased CCR2/NeuN immunoreactivity (Group C, $58\ 242.00 \pm 12\ 198.61$ vs Group D, $77\ 912.33 \pm 1277.77$, $p < .05$) in the dorsal horns of burn-injured rats. These results indicate that PRP can alleviate burn-induced neuropathic pain (Figure 5).

Subcutaneous PRP injection decreased p-JNK and p-NFκB immunoreactivity in astrocytes in spinal cord dorsal horns

To investigate the effects of PRP on p-JNK and p-NFκB activation in spinal cord dorsal horns, p-JNK, p-NFκB, and GFAP (which are central sensitization, inflammation, and astrocyte markers, respectively) were quantified through double immunofluorescence staining (Figure 6). Compared with the group C, the proportion of p-JNK/GFAP double-positive cells as well as p-NFκB/GFAP double-positive cells significantly decreased in the group D (group C $8.89\% \pm 1.57\%$ vs group D $2.08\% \pm 0.59\%$, $p < 0.01$, and group C $29.86 \pm 3.34\%$ vs group D $7.48\% \pm 2.73\%$, $p < 0.01$, respectively). In our finding, JNK and NFκB pathways are involved in the production of proinflammatory cytokines, which may in turn become neuroinflammation and neuropathic pain.

Discussion

In this study, we demonstrated that using subcutaneous PRP injection to treat burn-induced neuropathic pain alleviates neuropathic pain. This treatment strategy also improved the skin and spinal expression of neuropathic pain parameters. Our results demonstrate that PRP subcutaneous injection in burn-induced painful scar is potentially effective for ameliorating burn-induced neuropathic pain.

PRP a sample of autologous blood with platelet concentrations exceeding the baseline values is prepared by centrifugation. The platelet concentrations, activities, and yields in the PRP can thus differ depending on the centrifugation steps, forces, and iterations. In the United States, more than 10 commercial PRP preparation systems have been approved by the Food and Drug Administration in USA. In this study, we used the PRP tube produced by AesMed Co., Ltd., Taipei, Taiwan. Per our results, the platelet count and the PDGF-AA/BB, VEGF, and EGF concentration in the PRP were significantly higher than those in plasma (Table 1), confirming that the PRP used in this study has high concentrations of growth factors and platelet.

To our knowledge, no studies have yet reported on the effects of PRP in treating burn-induced neuropathic pain. PRP has been reported to function

as an anti-inflammatory agent that decreases proinflammatory mediators[23]. The anti-inflammatory effects of PRP are realized through a reduction of NFκB transactivation, a critical regulator of the inflammatory process[24, 25]. Our results were consistent with the known phenomenon that PRP local injection around scar areas reduced inflammation in spinal cord dorsal horns. Moreover, chondrogenesis studies have reported that PRP reduces the expression of inflammatory enzymes cyclooxygenase 2 and 4 (COX-2 and -4), also decreasing disintegrin and metalloproteinases with thrombospondin motifs gene expression [24, 26]. These reports all suggest that PRP has anti-inflammatory effects.

Our literature review revealed a lack of standardization for PRP dosing and treatment interval. Therefore, the outcomes of research evaluating the clinical effectiveness of PRP have been controversial. A knee osteoarthritis study suggested that PRP injections administered in 2 to 4 sessions, 2 to 4 weeks apart, are effective[23]. Furthermore, autologous PRP injections have been shown to have greater and longer efficacy than do hyaluronic acid injections in reducing pain and recovering articular function[27]. These results indicate that PRP exerts long-lasting anti-inflammatory effects. The magnitude and effectiveness of platelet concentration in the PRP varies depending on the preparation technique. Moreover, use of an activator, the presence of leukocytes in the PRP, application frequency, and the range of platelet count are all currently being debated. In addition, many studies have adopted short follow-up periods. In this study, PRP was prepared through a standardized method as suggested by the commercial manufacturer, and no filters were used; 1.1 billion–1.4 billion platelets were injected, 6-fold higher than the baseline value; this range, which is within the recommended range, is similar to that used in many studies (Table 1) [28, 29]. We injected 0.4ml PRP to the hind paw area, this injected volume was based on our previous study in fat graft injection and stem cell therapy[21, 30].

Zhang *et al.* found that the activation of spinal mTOR is a crucial component of chronic constriction injury (CCI) induced neuropathic pain[31]. The inhibition of the spinal mTOR pathway through the intrathecal injection of PRP can reduce mechanical allodynia, meaning that in neuropathic rats, the anti-nociceptive effects are based on the inhibition of the spinal mTOR pathway. In the present study, we observed the upregulation of p-mTOR following burn-induced neuropathic pain (Figure 3). Recent studies on the brain injury model and CCI model of the spinal cord have shown that PTEN is an upstream inhibitory mediator of mTOR in the central nervous

system [8, 32]. And exert of PTEN also had beneficial effects on anti-neuropathic pain, thus PTEN played an important role in a rodent model of neuropathic pain[8]. Our results indicate that burn injury-induced neuropathic pain decreased PTEN immunoreactivity in hind paw skin and spinal cord dorsal horns and

that subcutaneous PRP injection in the hind paw increased PTEN immunoreactivity in both areas while also decreasing mTOR immunoreactivity. Moreover, neuropathic mechanical allodynia in the hind paw was blocked by the subcutaneous PRP injection, and this effect lasted for more than 2 weeks (Figure 1).

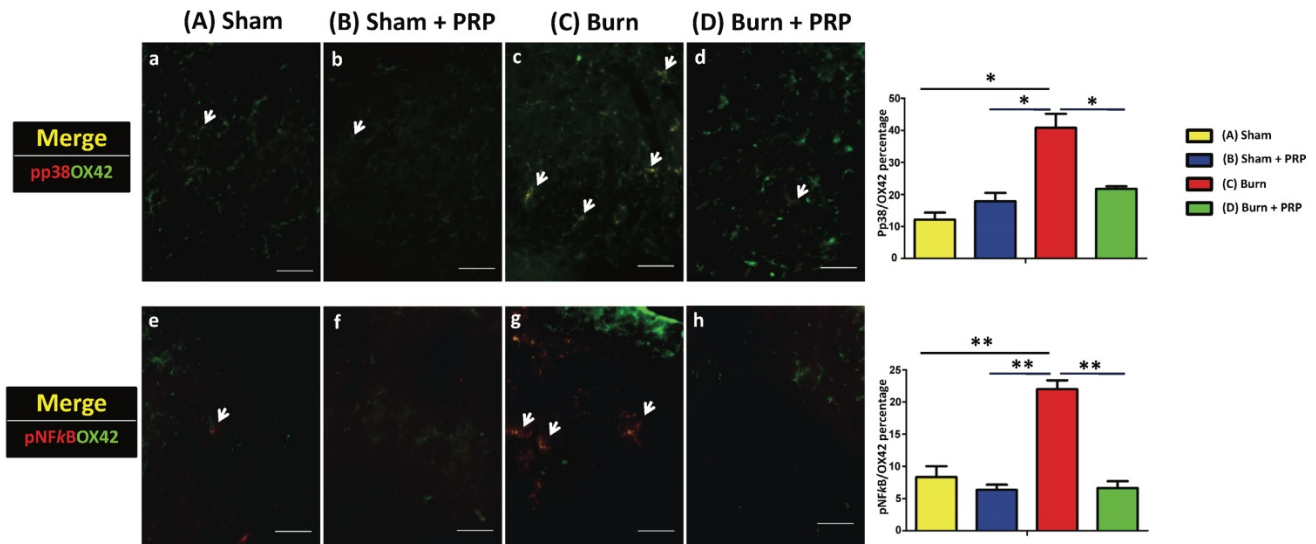


Figure 4. Subcutaneous PRP injection decreased p-p38 and p-NFκB immunoreactivity in spinal cord dorsal horns. Spinal cord sections (10 μm) were harvested 4 weeks after PRP injection. Double immunofluorescence staining was performed for p-p38 (red), p-NFκB (red), and OX42 (green, microglia cell). The total number of p-p38 and OX42 double-positive cells in the burn + PRP group decreased significantly compared with the burn group (p-p38/OX42, group C 40.76% ± 6.22% vs group D 21.72% ± 1.11%, $P < 0.05$). The number of p-NFκB-expressing microglia was significantly higher in the group C than in the group D (burn 21.96 ± 1.94%, burn + PRP 6.62 ± 1.51, $p < 0.01$). Scale bars in all images are 50 μm.

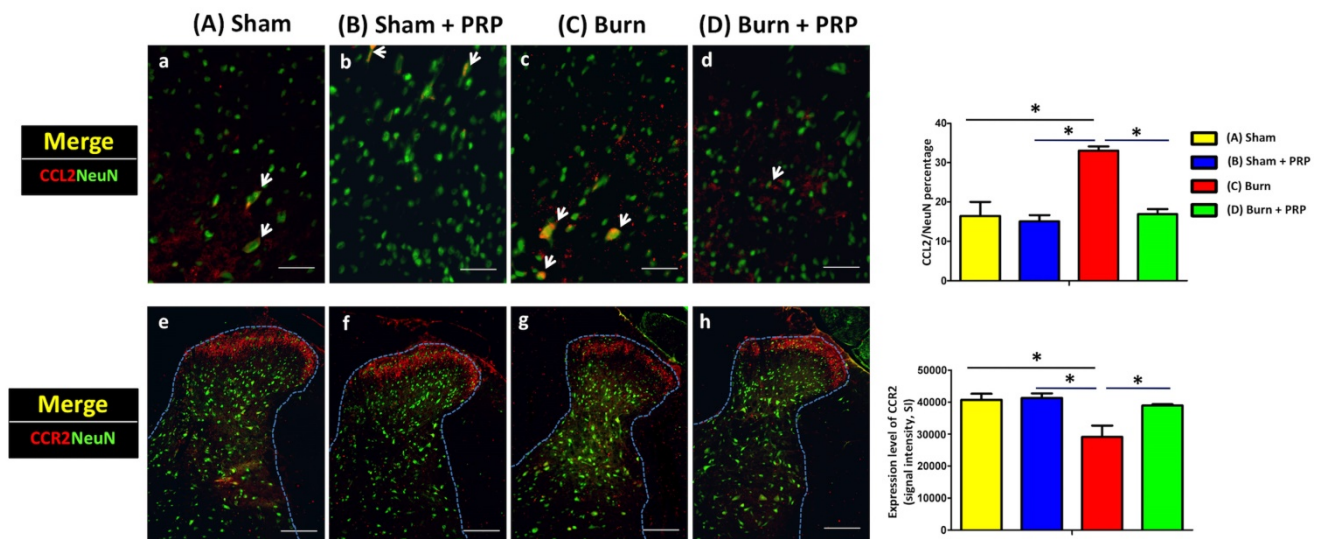


Figure 5. Subcutaneous PRP injection decreased CCL2/NeuN and increased CCR2/NeuN double-positive cell number in the dorsal horn for burn-induced neuropathic pain. Spinal cord sections (10 μm) were harvest 4 weeks after PRP injection. Arrows indicate representative double-positive cells in the dorsal horn. Subcutaneous PRP injection significantly decreased CCL2 immunoreactivity (group C 33.05 ± 1.49% vs group D 16.87% ± 1.86%, $p < .05$) and significantly increased CCR2/NeuN immunoreactivity (Group C, 58 242.00 ± 12 198.61 vs Group D, 77 912.33 ± 1277.77, $p < .05$) in the dorsal horn of burn-injured rats. CCL2 and CCR2 scale bars are 50 and 200 μm, respectively.

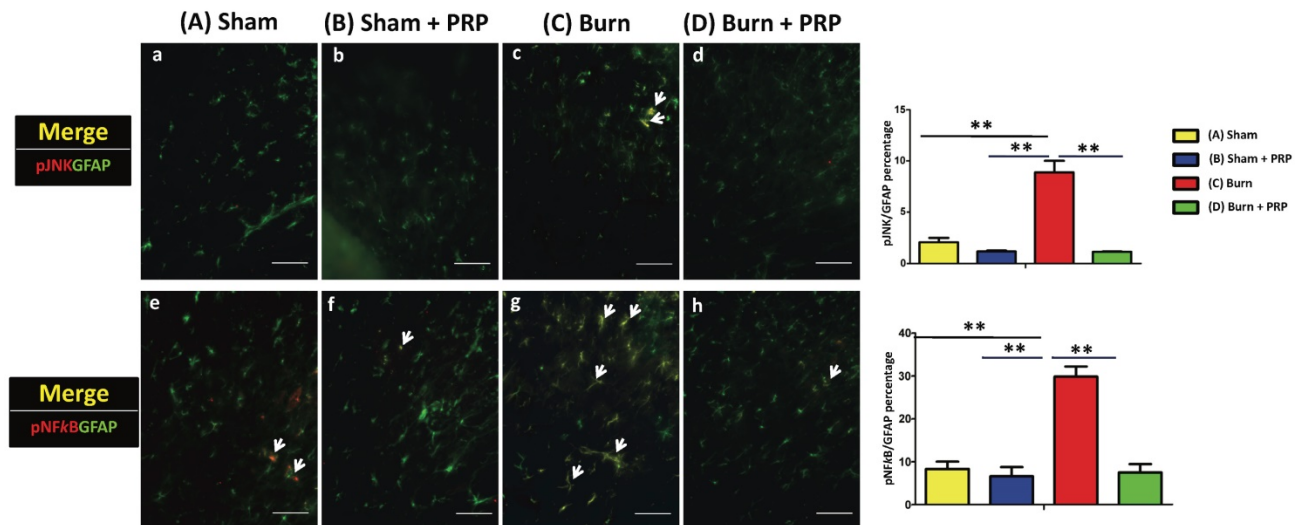


Figure 6. Subcutaneous PRP injection decreased p-JNK and p-NFκB immunoreactivity in astrocytes in spinal cord dorsal horns. Spinal cord sections (10 μm) were harvest 4 weeks after PRP injection. Double immunofluorescence staining was performed for p-JNK (red), p-NFκB (red), and GFAP (green, astrocyte). The proportion of p-JNK/GFAP double-positive cells significantly decreased in the group C (group C $8.89\% \pm 1.57\%$ vs group D $2.08\% \pm 0.59\%$, $p < 0.01$), and the proportion of p-NFκB/GFAP double-positive cells significantly decreased in the group D compared with the group C (group D $7.48\% \pm 2.73\%$ vs group C $29.86\% \pm 3.34\%$ $P < 0.01$). Scale bars in all images are 50 μm.

In the nerve injury model, persistent pain is facilitated by increased astrocyte and microglial activation and upregulation of inflammatory cytokines IL-1β and TNF-α.[33] The selective cellular localization of CCL2 observed in the present study suggests that neuronal activation after burn injury leads to secretion of the CCL2 chemokine, which in turn results in central sensitization and hypersensitivity; following PRP injection, CCR2 is downregulated significantly.[12] Other possible mechanisms for CCL2-induced pain facilitation such as CCL2-induced hyperalgesia and CCR2 expression in neurons at the spinal level and enhancement of NMDA-induced current in spinal neurons by CCL2 should also be considered.[12] Furthermore, CCR2 may interact with NMDA receptors in neurons in pain pathways. In summary, the effects of CCL2/CCR2 signaling are responsible for persistent neuropathic pain,[34] and PRP injection downregulates CCL2 expression.

Conclusions

PRP reduced p-PTEN, p-mTOR, and CCL2 expressions in neuron cells. Furthermore, it also decreased p-p38 and p-NFκB expressions in microglia and p-JNK and p-NFκB activation in spinal astrocytes, indicating attenuated inflammation. Our findings thus provide evidence that PRP, because of its anti-inflammatory effects, can be used as an alternative therapeutic method for treating burn-induced neuropathic pain.

Acknowledgments

This work was supported by grants from the Ministry of Science and Technology of Taiwan (MOST 104-2314-B-037-061-MY3, MOST106-2314-B-037-028, MOST 104-2221-E-005-096-MY2 and MOST 104-2628-E-005-004-MY3); Kaohsiung Medical University 'Aim for the Top Universities Grant' (KMU-TP105 G00, KMU-TP105G02, KMU-TP105B07), Kaohsiung Medical University Hospital (KMUH 105-5R69), and Childhood Burn Foundation of the Republic of China. We also gratefully acknowledge Miss Yen-Hsin Kuo for providing technical assistance and preparing the figures in this article.

Competing Interests

The authors have declared that no competing interest exists.

References

1. Peck MD. Epidemiology of burns throughout the world. Part I: Distribution and risk factors. *Burns*. 2011; 37: 1087-1100.
2. Malenfant A, Forget R, Amsel R, et al. Tactile, thermal and pain sensibility in burned patients with and without chronic pain and paresthesia problems. *Pain*. 1998; 77: 241-251.
3. Forbes-Duchart L, Cooper J, Nedelec B, et al. Burn therapists' opinion on the application and essential characteristics of a burn scar outcome measure. *J Burn Care Res*. 2009; 30: 792-800.
4. Dauber A, Osgood PF, Breslau AJ, et al. Chronic persistent pain after severe burns: a survey of 358 burn survivors. *Pain Med*. 2002; 3: 6-17.
5. Summer GJ, Puntillo KA, Miaskowski C, et al. Burn injury pain: the continuing challenge. *J Pain*. 2007; 8: 533-548.
6. Dworkin RH, O'Connor AB, Kent J, et al. Interventional management of neuropathic pain: NeuPSIG recommendations. *Pain*. 2013; 154: 2249-2261.
7. Finnerup NB, Attal N, Haroutounian S, et al. Pharmacotherapy for neuropathic pain in adults: a systematic review and meta-analysis. *Lancet Neurol*. 2015; 14: 162-173.
8. Huang SY, Sung CS, Chen WF, et al. Involvement of phosphatase and tensin homolog deleted from chromosome 10 in rodent model of neuropathic pain. *J Neuroinflammation*. 2015; 12: 59.

9. Calvo M, Dawes JM, Bennett DL. The role of the immune system in the generation of neuropathic pain. *Lancet Neurol.* 2012; 11: 629-642.
10. Liu T, Gao YJ, Ji RR. Emerging role of Toll-like receptors in the control of pain and itch. *Neurosci Bull.* 2012; 28: 131-144.
11. Gao YJ and Ji RR. Chemokines, neuronal-glia interactions, and central processing of neuropathic pain. *Pharmacol Ther.* 2010; 126: 56-68.
12. Guo W, Wang H, Zou S, et al. Chemokine signaling involving chemokine (C-C motif) ligand 2 plays a role in descending pain facilitation. *Neurosci Bull.* 2012; 28: 193-207.
13. Padi SS, Shi XQ, Zhao YQ, et al. Attenuation of rodent neuropathic pain by an orally active peptide, RAP-103, which potently blocks CCR2- and CCR5-mediated monocyte chemotaxis and inflammation. *Pain.* 2012; 153: 95-106.
14. Raeissadat SA, Rayegani SM, Hassanabadi H, et al. Knee Osteoarthritis Injection Choices: Platelet- Rich Plasma (PRP) Versus Hyaluronic Acid (A one-year randomized clinical trial). *Clin Med Insights Arthritis Musculoskelet Disord.* 2015; 8: 1-8.
15. Sriram S, Sankaralingam R, Mani M, et al. Autologous platelet rich plasma in the management of non-healing vasculitic ulcers. *Int J Rheum Dis.* 2016;
16. Giannoudis PV, Hak D, Sanders D, et al. Inflammation, Bone Healing, and Anti-Inflammatory Drugs: An Update. *J Orthop Trauma.* 2015; 29 Suppl 12: S6-9.
17. Knezevic NN, Candido KD, Desai R, et al. Is Platelet-Rich Plasma a Future Therapy in Pain Management? *Med Clin North Am.* 2016; 100: 199-217.
18. Fitzpatrick J, Bulsara M, Zheng MH. The Effectiveness of Platelet-Rich Plasma in the Treatment of Tendinopathy: A Meta-analysis of Randomized Controlled Clinical Trials. *Am J Sports Med.* 2016;
19. Montanez-Heredia E, Irizar S, Huertas PJ, et al. Intra-Articular Injections of Platelet-Rich Plasma versus Hyaluronic Acid in the Treatment of Osteoarthritic Knee Pain: A Randomized Clinical Trial in the Context of the Spanish National Health Care System. *Int J Mol Sci.* 2016; 17:
20. Kuffler DP. Platelet-rich plasma and the elimination of neuropathic pain. *Mol Neurobiol.* 2013; 48: 315-332.
21. Huang SH, Wu SH, Chang KP, et al. Autologous fat grafting alleviates burn-induced neuropathic pain in rats. *Plast Reconstr Surg.* 2014; 133: 1396-1405.
22. Huang SH, Wu SH, Lee SS, et al. Fat Grafting in Burn Scar Alleviates Neuropathic Pain via Anti-Inflammation Effect in Scar and Spinal Cord. *PLoS One.* 2015; 10: e0137563.
23. Meheux CJ, McCulloch PC, Lintner DM, et al. Efficacy of Intra-articular Platelet-Rich Plasma Injections in Knee Osteoarthritis: A Systematic Review. *Arthroscopy.* 2016; 32: 495-505.
24. Kabiri A, Esfandiari E, Esmaili A, et al. Platelet-rich plasma application in chondrogenesis. *Adv Biomed Res.* 2014; 3: 138.
25. Bendinelli P, Matteucci E, Dogliotti G, et al. Molecular basis of anti-inflammatory action of platelet-rich plasma on human chondrocytes: mechanisms of NF-kappaB inhibition via HGF. *J Cell Physiol.* 2010; 225: 757-766.
26. Pereira RC, Scaranari M, Benelli R, et al. Dual effect of platelet lysate on human articular cartilage: a maintenance of chondrogenic potential and a transient proinflammatory activity followed by an inflammation resolution. *Tissue Eng Part A.* 2013; 19: 1476-1488.
27. Kon E, Mandelbaum B, Buda R, et al. Platelet-rich plasma intra-articular injection versus hyaluronic acid viscosupplementation as treatments for cartilage pathology: from early degeneration to osteoarthritis. *Arthroscopy.* 2011; 27: 1490-1501.
28. Zhang Y, Morgan BJ, Smith R, et al. Platelet-rich plasma induces post-natal maturation of immature articular cartilage and correlates with LOXL1 activation. *Sci Rep.* 2017; 7: 3699.
29. Everts PA, Knape JT, Weibrich G, et al. Platelet-rich plasma and platelet gel: a review. *J Extra Corpor Technol.* 2006; 38: 174-187.
30. Wu SH, Huang SH, Lo YC, et al. Autologous adipose-derived stem cells attenuate muscular atrophy and protect spinal cord ventral horn motor neurons in an animal model of burn injury. *Cytotherapy.* 2015; 17: 1066-1075.
31. Zhang W, Sun XF, Bo JH, et al. Activation of mTOR in the spinal cord is required for pain hypersensitivity induced by chronic constriction injury in mice. *Pharmacol Biochem Behav.* 2013; 111: 64-70.
32. Shi GD, OuYang YP, Shi JG, et al. PTEN deletion prevents ischemic brain injury by activating the mTOR signaling pathway. *Biochem Biophys Res Commun.* 2011; 404: 941-945.
33. Roberts J, Ossipov MH, Porreca F. Glial activation in the rostroventromedial medulla promotes descending facilitation to mediate inflammatory hypersensitivity. *Eur J Neurosci.* 2009; 30: 229-241.
34. Sonekatsu M, Taniguchi W, Yamanaka M, et al. Interferon-gamma potentiates NMDA receptor signaling in spinal dorsal horn neurons via microglia-neuron interaction. *Mol Pain.* 2016; 12: